Support Information

Carbon Intercalated $Ti_3C_2T_x$ MXene for High-Performance Electrochemical Energy Storage

Lei Shen,[a,b] Xiaoya Zhou,[a] Xinglin Zhang,[a] Yizhou Zhang,[a] Yunlong Liu,[c] Wenjun Wang,[c] Weili Si,*[a] Xiaochen Dong*[a]

[a]Key Laboratory of Flexible Electronics (KLOFE) & Institute of Advanced Materials (IAM), Nanjing Tech University (NanjingTech), 30 South Puzhu Road, Nanjing 211800, China. E-mail: iamxcdong@njtech.edu.cn; iamwlsi@njtech.edu.cn

[b]Department of Chemistry & Materials Engineering, Jiangsu Key Laboratory of Advanced Functional Materials, Changshu Institute of Technology, Changshu 215500, China.

[c]School of Physical Science and Information Technology, Liaocheng University, Shandong 252059, China.

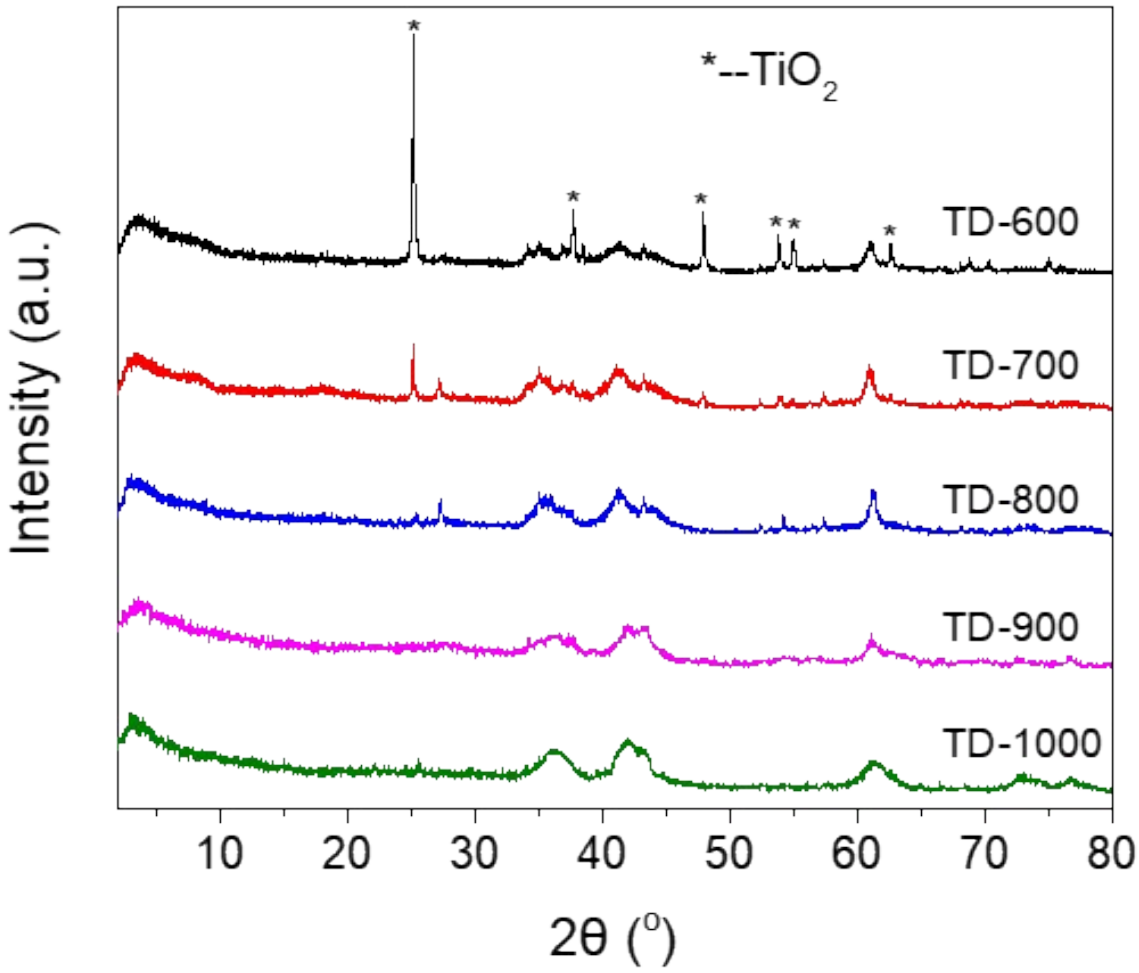

Figure S1a. XRD patterns of TD-600, TD-700, TD-800, TD-900 and TD-1000, respectively.

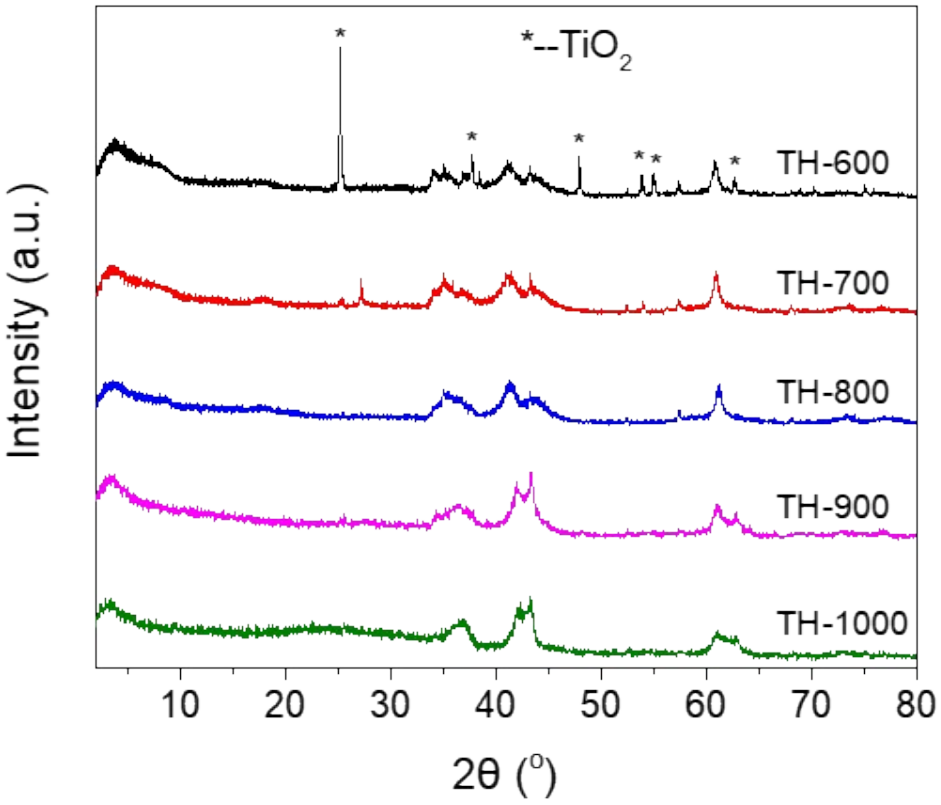

Figure S1b. XRD patterns of TH-600, TH-700, TH-800, TH-900 and TH-1000, respectively.

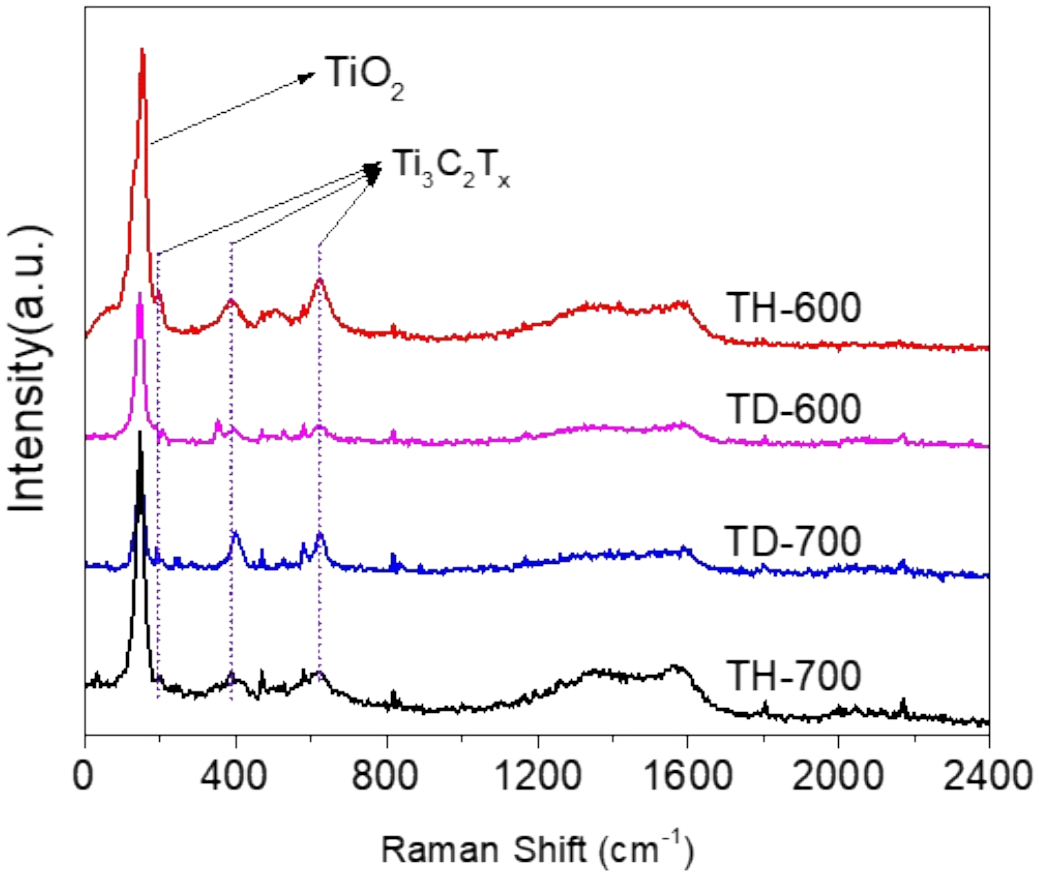

Figure S2. Raman spectra of TD-600, TD-700, TH-600 and TH-700, respectively.

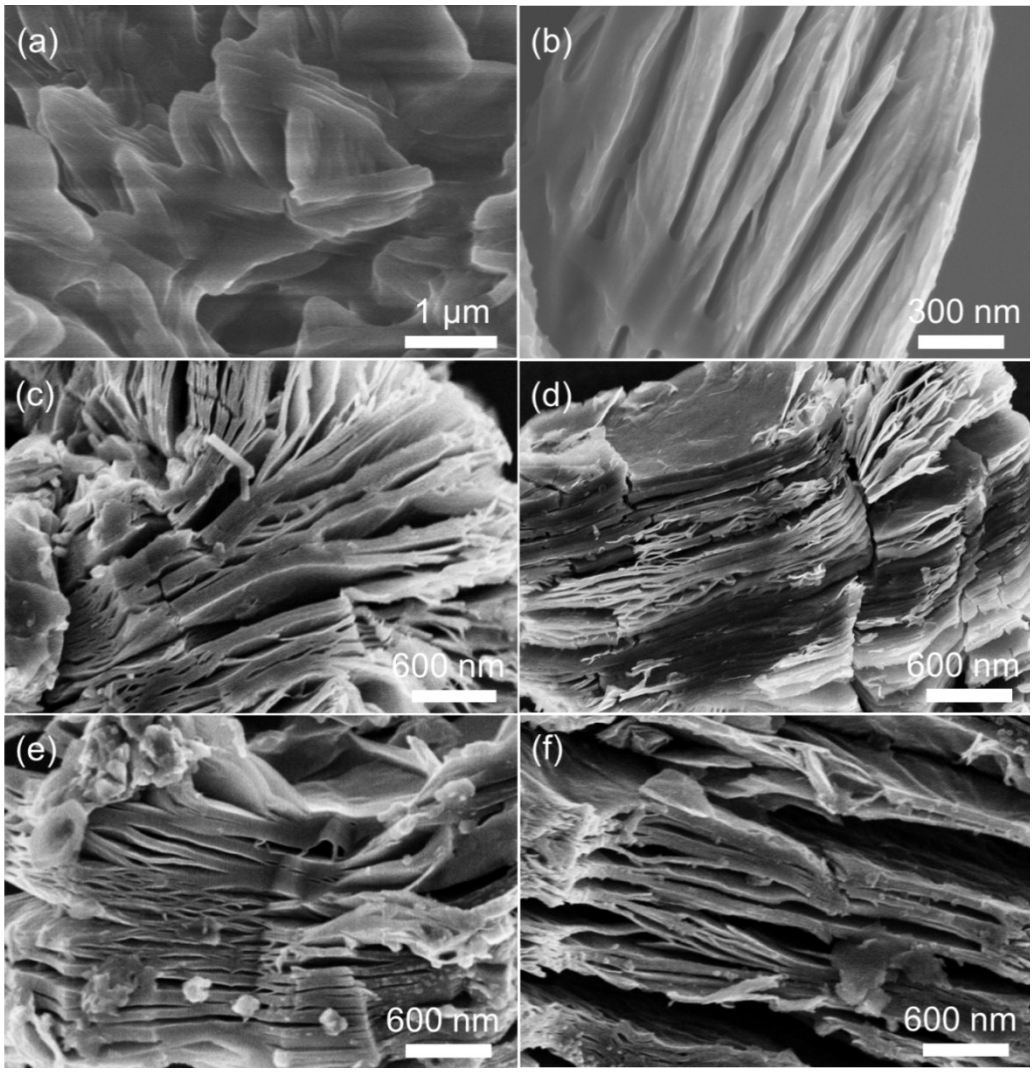

Figure S3. SEM images of (a-b) $Ti_3C_2T_x$-DDA, (c) TD-600, (d) TD-700, (e) TH-600, (f) TH-700.

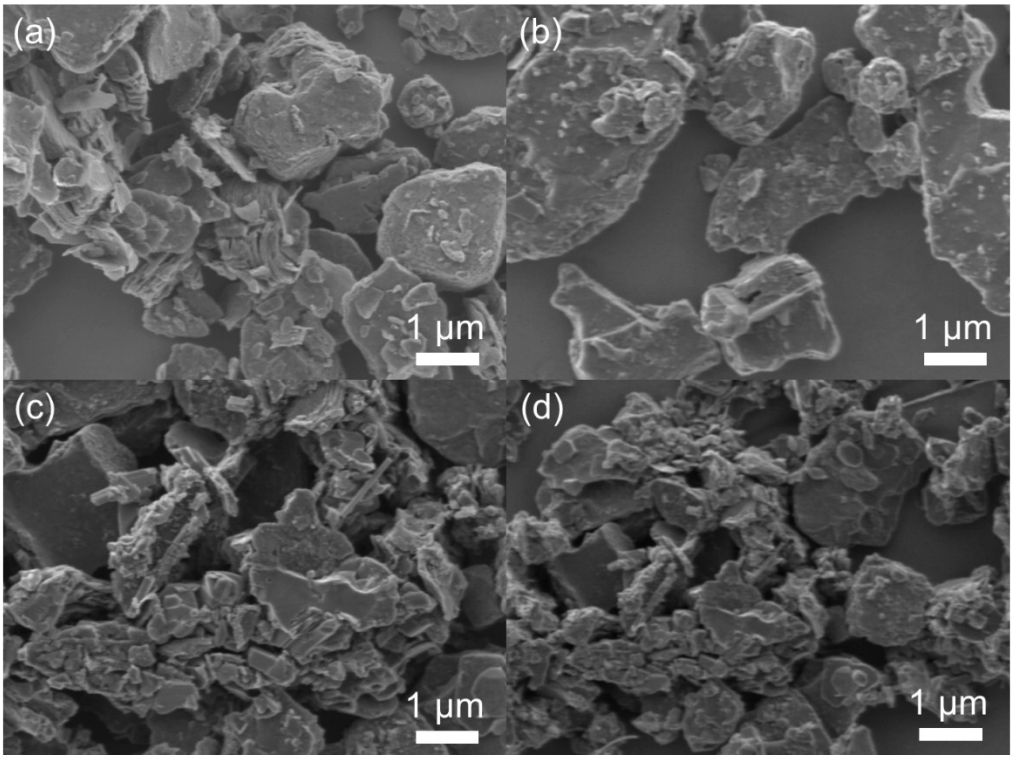

Figure S4. SEM images of (a) TH-900, (b) TD-900, (c) TH-1000, (d) TD-1000.

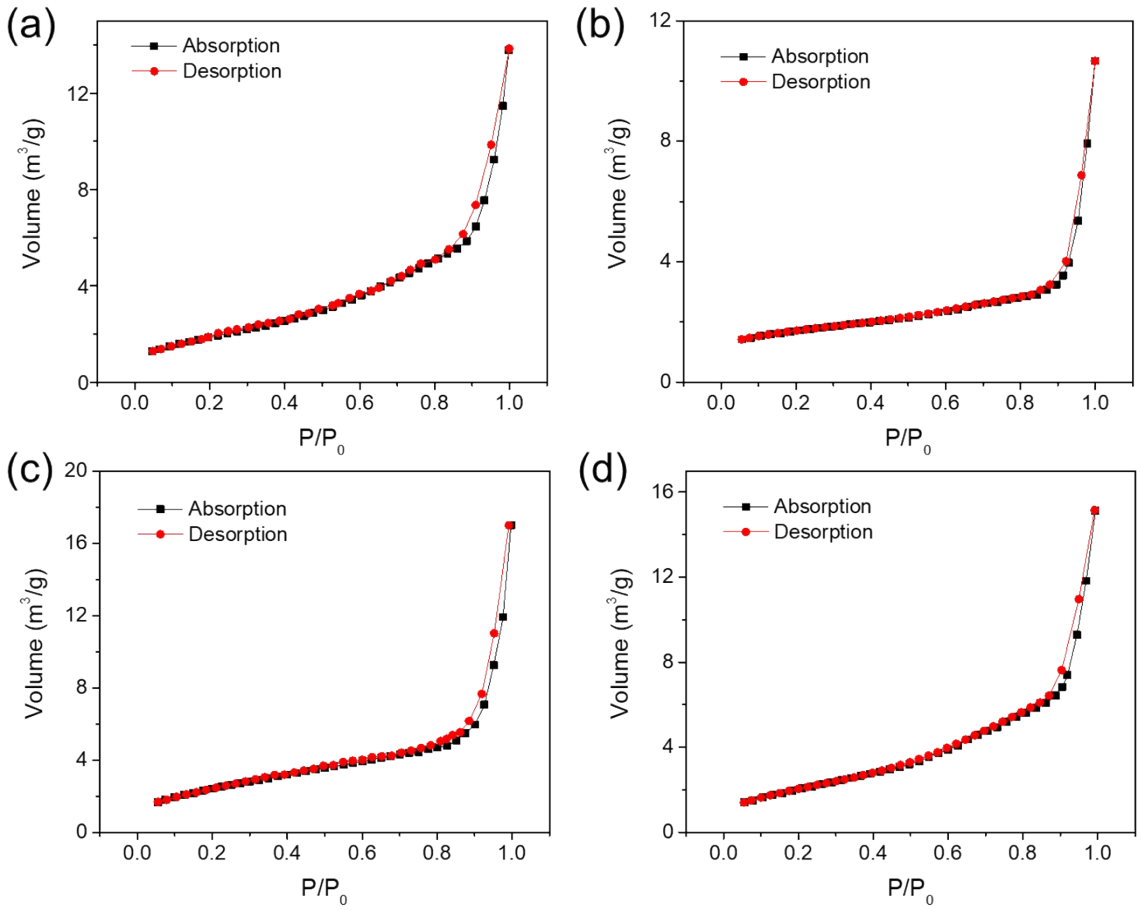

Figure S5. N2 adsorption-desorption isotherms of (a) $Ti_3C_2T_x$, (b) $Ti_3C_2T_x$ -800, (c) TH-800 and (d) TD-800

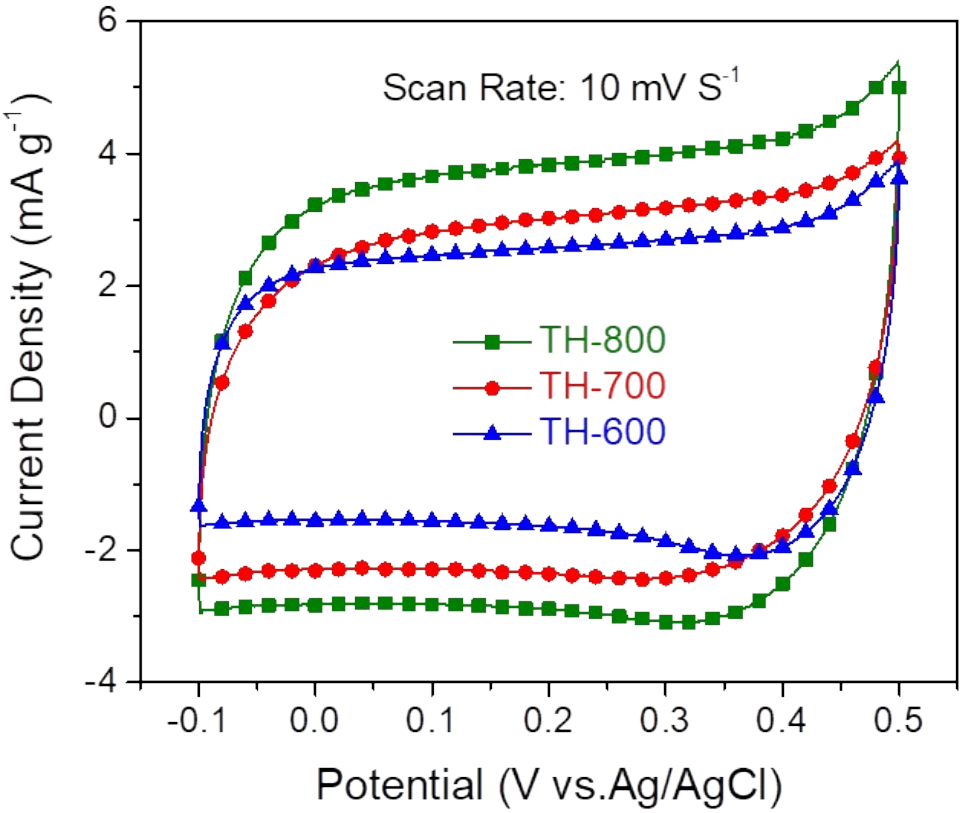

Figure S6. CV curves of TH-800, TH-700, and TH-600 electrodes (scan rates 10 mV s^{-1}).

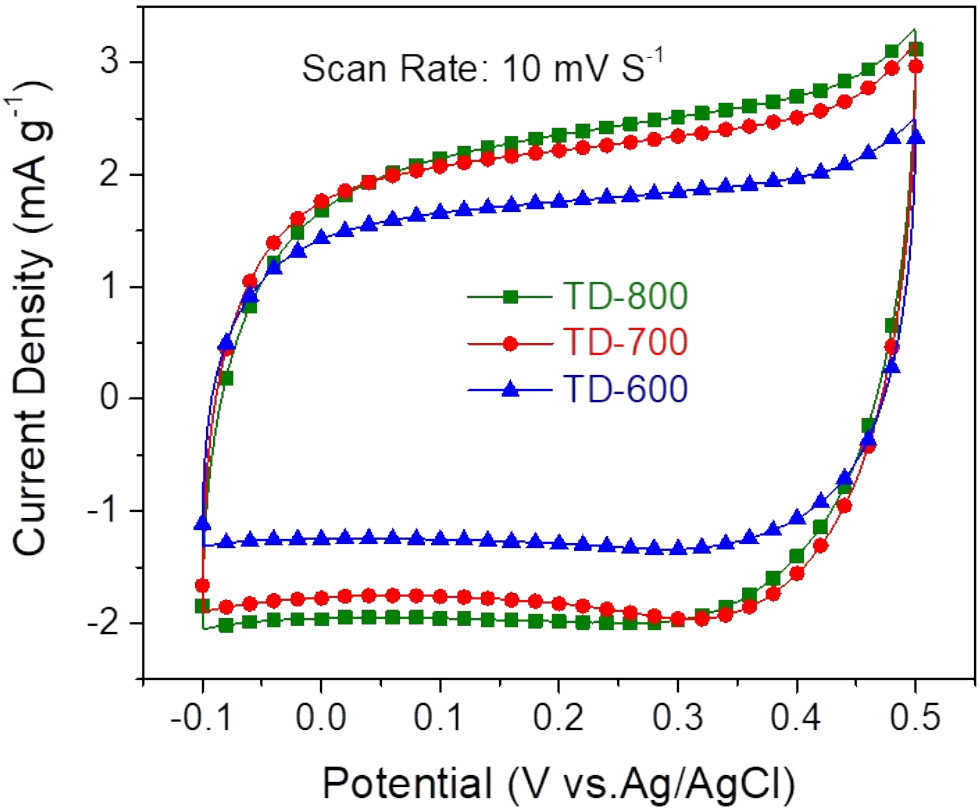

Figure S7. CV curves of TD-800, TD-700 and TD-600 electrodes (scan rates 10 mV s^{-1}).

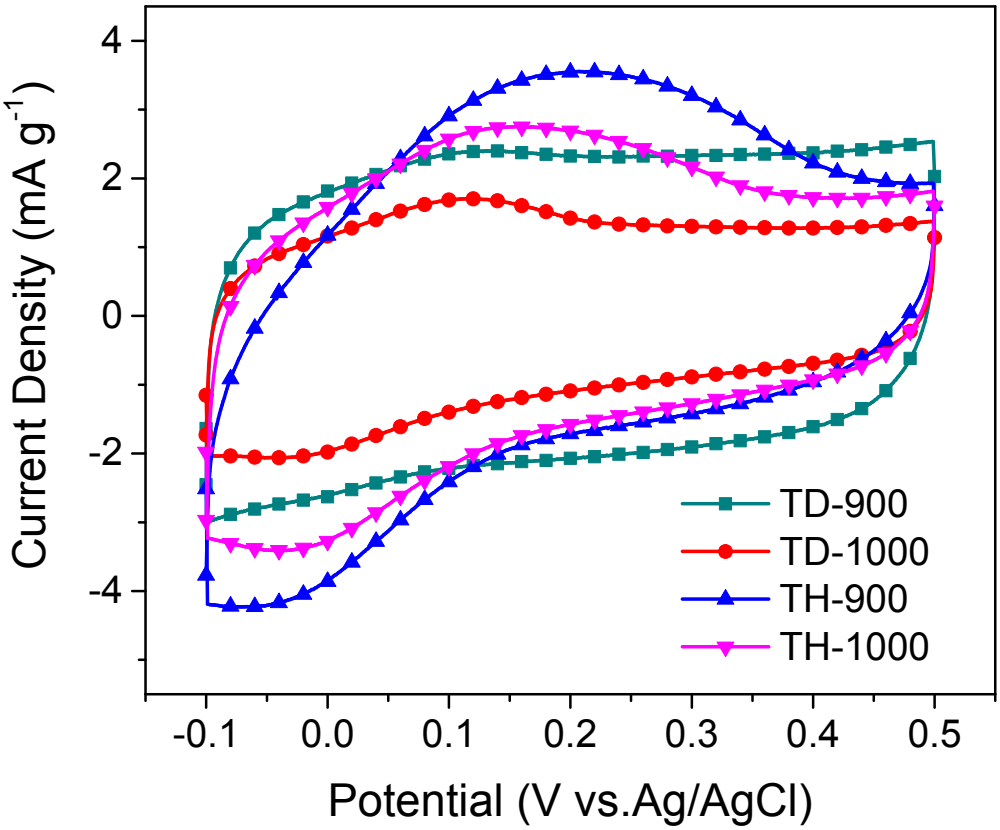

Figure S8. CV curves of TD-900, TD-1000, TH-900 and TH-1000 electrodes (scan rates 10 mV s^{-1}).

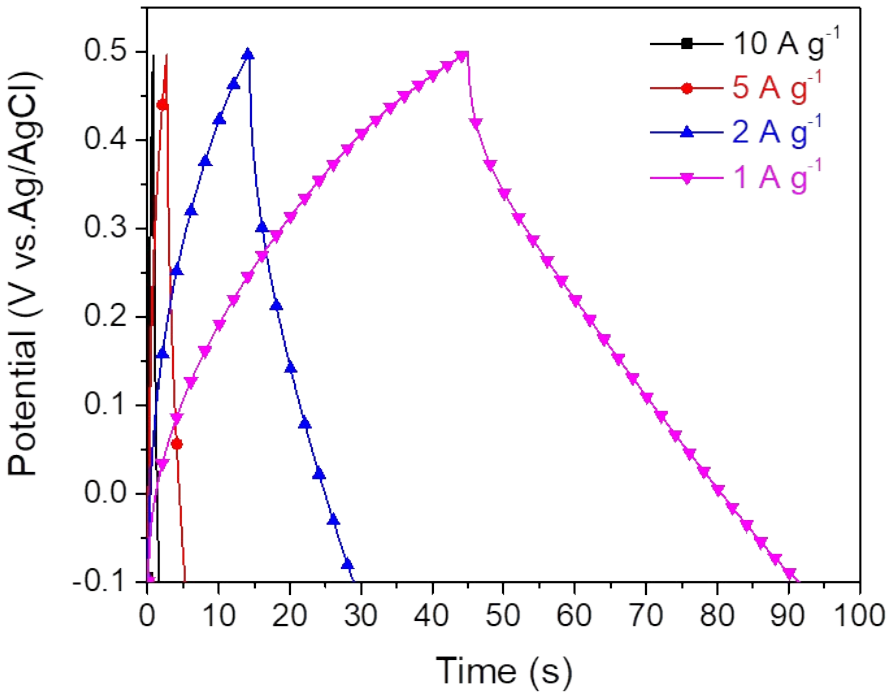

Figure S9. GCD curves of $Ti_3C_2T_x$ electrode in the potential window from -0.1 V to 0.5 V at different current densities (1, 2, 5 and 10 Ag^{-1}).

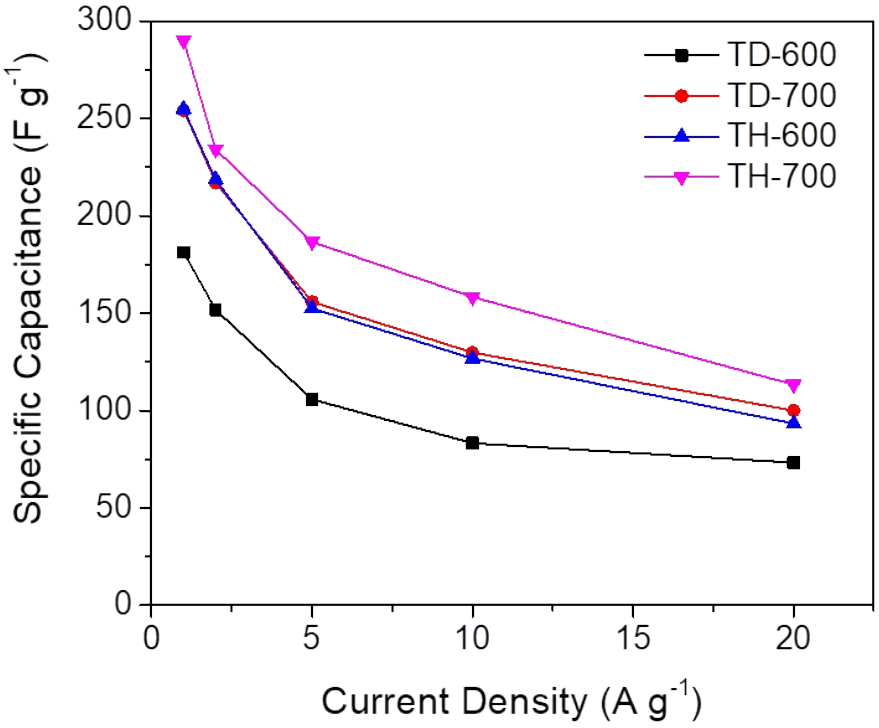

Figure S10. Rate performance of TH-600, TH-700, TD-600, and TD-700 electrodes as the function of scan rate.

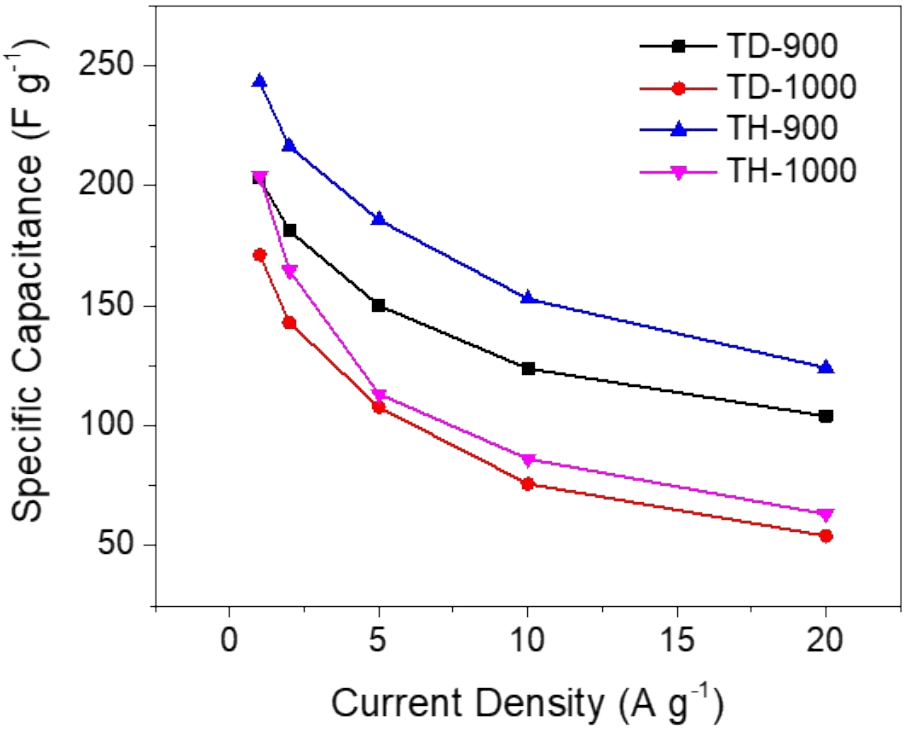

Figure S11. Rate performance of TD-900, TD-1000, TH-900 and TH-1000 electrodes as the function of scan rate.

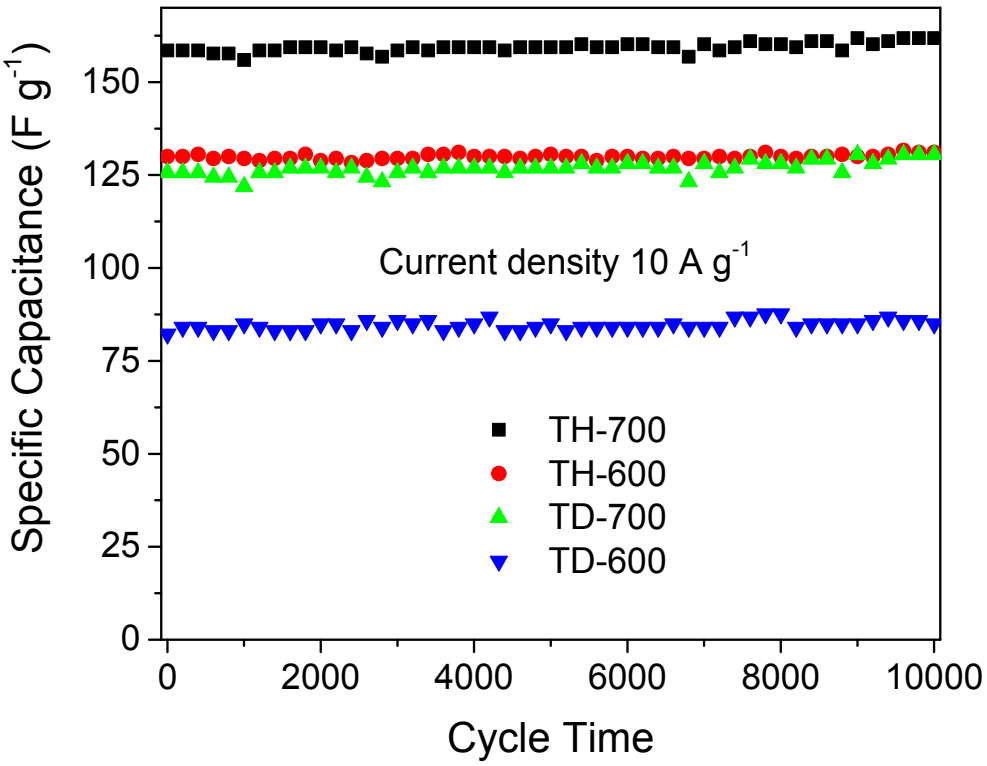

Figure S12. Capacitance retention tests of TH-600, TH-700, TD-600, and TD-700 electrodes in H_2SO_4.

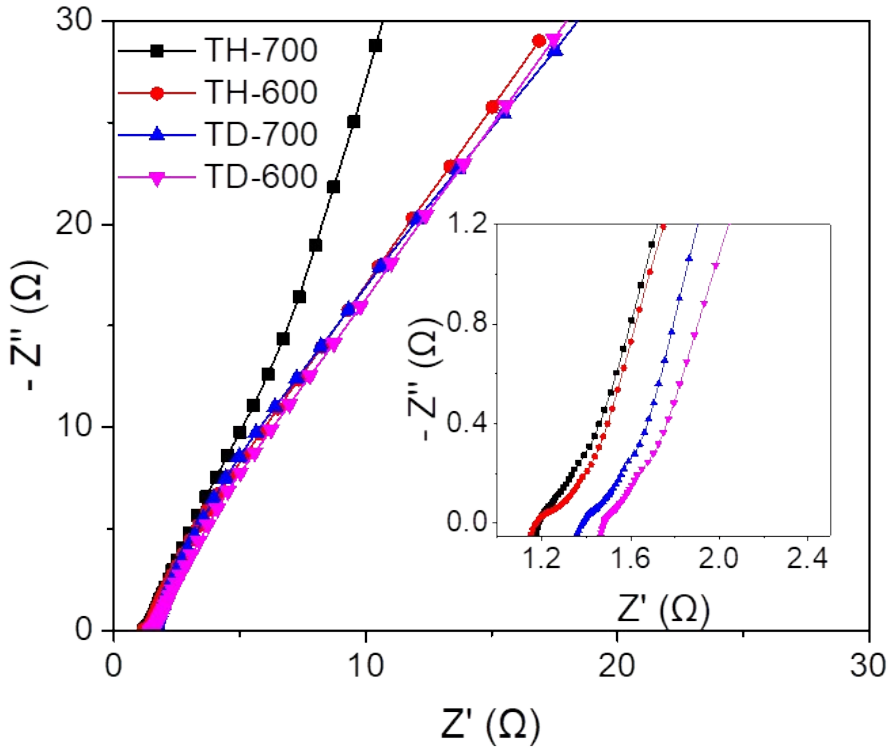

Figure S13. EIS curves in H_2SO_4 for TH-600, TH-700, TD-600 and TD-700 electrodes. Inset shows the magnified high-frequency region.

Table S1 Comparison of specific capacitance and cycle performance with reported MXene-based composites electrodes

Materials	Capacitance	Cycling	Ref
$Ti_3C_2T_x$/carbon nanotubes	85 F g^{-1} (1 A g^{-1})	90% (1000)	[1]
$Ti_3C_2T_x$/single-walled carbon nanotubes	220 mF cm^{-2} (2 mV s^{-1})	95% (10000)	[2]
Mo_2CT_x	196 F g^{-1} (2 mV s^{-1})	100% (10000)	[3]
400-KOH-Ti_3C_2	517 F g^{-1} (1 A g^{-1})	100% (10000)	[4]
Macroporous $Ti_3C_2T_x$	380 F g^{-1} (2 mV s^{-1})	90% (10000)	[5]
Hydrazine intercalation into $Ti_3C_2T_x$	250 F g^{-1} (10 mV s^{-1})	100% (10000)	[6]
MnO_2/$Ti_3C_2T_x$	210.9 F g^{-1} (10 mV s^{-1})	88% (10000)	[7]
Ti_3C_2-(After HF etching of 216h)	118 F g^{-1} (5 mV s^{-1})	100% (5000)	[8]
MnO_2-Ti_3C_2	377 mF cm^{-2} (5 mV s^{-1})	95% (5000)	[9]
N-$Ti_3C_2T_x$-200 °C	192 F g^{-1} (1 mV s^{-1})	-	[10]
$Ti_3C_2T_x$/MWCNT	150 F g^{-1} (2 mV s^{-1})	100% (10000)	[11]
Polymerization pyrrole confined $Ti_3C_2T_x$	416 F g^{-1} (5 mV s^{-1})	92% (25000)	[12]
Poly(9,9-dioctylfluorene)/$Ti_3C_2T_x$	380 F g^{-1} (2 mV s^{-1})	100% (10000)	[13]
$Ti_3C_2T_x$	245 F g^{-1} (2 mV s^{-1})	100% (10000)	[14]
This Work	364.3 F g^{-1} (1 A g^{-1})	100% (10000)	

Reference

[1] Y. Dall'Agnese, P. Rozier, P.-L. Taberna, Y. Gogotsi, P. Simon, *J. Power Sources* **2016**, *306*, 510.

[2] Q. Fu, X. Wang, N. Zhang, J. Wen, L. Li, H. Gao, X. Zhang, *J. Colloid Interf. Sci.* **2018**, *511*, 128.

[3] J. Halim, S. Kota, M. R. Lukatskaya, M. Naguib, M.-Q. Zhao, E. J. Moon, J. Pitock, J. Nanda, S. J. May, Y. Gogotsi, M. W. Barsoum, *Adv. Funct. Mater.* **2016**, *26*, 3118.

[4] J. Li, X. Yuan, C. Lin, Y. Yang, L. Xu, X. Du, J. Xie, J. Lin, J. Sun, *Adv. Energy Mater.* **2017**, *7*, 1602725.

[5] M. R. Lukatskaya, S. Kota, Z. Lin, M.-Q. Zhao, N. Shpigel, M. D. Levi, J. Halim, P.-L. Taberna, M. W. Barsoum, P. Simon, Y. Gogotsi, *Nat. Energy* **2017**, *2*, 17105.

[6] O. Mashtalir, M. R. Lukatskaya, A. I. Kolesnikov, E. Raymundo-Pinero, M. Naguib, M. W. Barsoum, Y. Gogotsi, *Nanoscale* **2016**, *8*, 9128.

[7] R. B. Rakhi, B. Ahmed, D. Anjum, H. N. Alshareef, *ACS Appl. Mater. Interfaces* **2016**, *8*, 18806.

[8] Y. Tang, J. Zhu, C. Yang, F. Wang, *J. Electrochem. Soc.* **2016**, *163*, A1975.

[9] Y. Tang, J. Zhu, C. Yang, F. Wang, *J. Alloy. Compd.* **2016**, *685*, 194.

[10] Y. Wen, T. E. Rufford, X. Chen, N. Li, M. Lyu, L. Dai, L. Wang, *Nano Energy* **2017**, *38*, 368.

[11] M. Q. Zhao, C. E. Ren, Z. Ling, M. R. Lukatskaya, C. Zhang, K. L. Van Aken, M. W. Barsoum, Y. Gogotsi, *Adv. Mater.* **2015**, *27*, 339.

[12] M. Boota, B. Anasori, C. Voigt, M. Q. Zhao, M. W. Barsoum, Y. Gogotsi, *Adv. Mater.* **2016**, *28*, 1517.

[13] M. Boota, M. Pasini, F. Galeotti, W. Porzio, M.-Q. Zhao, J. Halim, Y. Gogotsi, *Chem. Mater.* **2017**, *29*, 2731.

[14] M. Ghidiu, M. R. Lukatskaya, M.-Q. Zhao, Y. Gogotsi, M. W. Barsoum, *Nature* **2014**, *516*, 78.